



3D-printed biomimetic bone implant polymeric composite scaffolds

Bankole Oladapo^{1,2} · Abolfazl Zahedi² · Sikiru Ismail⁴ · Wattala Fernando¹ · Omolayo Ikumapayi³

Received: 30 December 2022 / Accepted: 27 March 2023
© The Author(s) 2023

Abstract

This research introduced a new poly-ether-ether-ketone calcium hydroxyapatite (PEEK-cHAp) composite for a convenient, fast, and inexpensive femur bone-implant scaffold with different lattice structures to mimic natural bone structure. Fused deposition modelling (FDM) was used to print a hybrid PEEK-based filament-bearing bioactive material suited for developing cHAp. Using FDM, the same bone scaffold PEEK will be fabricated, depending on the shape of the bone fracture. The scaffolds were examined for in vitro bioactivity by immersing them in a simulated bodily fluid (SBF) solution. Furthermore, in vitro cytotoxicity tests validated the suitability of the composite materials employed to create minimal toxicity of the scaffolds. After spreading PEEK nanoparticles in the grains, the suggested spherical nanoparticle cell expanded over time. The motif affected the microstructure of PEEK-cHAp in terms of grain size and 3D shape. The results established the proposed optimum design and suitable material for prospective bone implants, as required for biomimetic artificial bone regeneration and healing.

Keywords Polymeric composites · FDM · Nanoparticles · Cell growth

1 Introduction

Bone regeneration is an exciting topic for many researchers [1–3]. Congenital and acquired diseases, such as trauma, infection, tumours, and failed arthroplasty, can result in bone defects that are too large for the body to heal. The patients frequently require invasive surgery to recover [1, 2]. Bone substitutes, such as polymeric scaffolds composite, stabilise bone growth. Consequently, bone is the second most frequent form of tissue transplanted globally; each year, at least four million procedures use bone grafts and substitutes [3, 4].

Recently, there has been significant research in interest in polymer-based bone tissue engineering structure (BTES),

particularly when natural and synthetic polymers are combined to create new scaffolds for tissue engineering. Bone tissue includes water, organic matter, and salt originating from living organisms [5, 6]. The best BTES must be structurally identical to the original bone tissue. At the same time, biocompatible and biodegradable natural polymers have low mechanical strength and thermal stability [7, 8]. Synthetic polymers, on the other side, have perfect mechanical properties, but their hydrophobic surfaces make fusing with the bone implant challenging. For example, gelatine can mimic the biological properties of natural bone matrix protein, but it is not particularly robust. Electrospinning and polymers can create tissue scaffolds with good biological and mechanical properties [8–10].

Moving forward, biomaterials have been used in various applications throughout history [10, 11]; for this study, they can be defined as any mixture of substances other than drugs that can interact with biological methods to heal, enhance, and replace tissues and bodily functions [6, 11, 12]. The most crucial requirements include the following: they permit cell development and proliferation, biodegrade at rates equivalent to the growth of the original tissue, are biocompatible, can provide growth factors, and have acceptable mechanical qualities in the proper forms. Additionally, biomaterials can be divided into three categories: (i)

✉ Bankole Oladapo
boladapo001@dundee.ac.uk

¹ School of Science and Engineering, University of Dundee, Dundee, United Kingdom

² Sustainable Development, De Montfort University, Leicester, United Kingdom

³ Mechanical Mechatronics Engineering, Afe Babalola University, Ado-Ekiti, Nigeria

⁴ School of Physics, Engineering and Computer Science, University of Hertfordshire, AL10 9AB Hatfield, United Kingdom

bioactive after implantation, (ii) bioresorbable and bioinert, and (iii) when there is little interaction with the surrounding tissues [13–15]. Bioactive after implantation refers to situations where a specific biological response at the biomaterial interface causes a bond between the tissue and the material. A beehive's hexagonal structure, a spider's web form, or hedgehog spines are only a few examples of natural models that inspired the design of biomimetics [16–18]. Among the most often used biomaterials can be found in metals, polymers, ceramics, or a combination of these materials. Because of their mechanical properties, metals may replace hard tissues, such as hip joints, with teeth and bone plates. Titanium and stainless steel are the most common metallic biomaterials. A main disadvantage of metallic biomaterial is that some of them, such as nickel, chromium, and cobalt, are toxic. Bioceramics are differentiated by their stiffness, hardness, and resistance to corrosion and wear [19–21].

There are significant challenges with using biomaterials that need to be addressed for destructive bone diseases. The gold treatment is autografts. Bone implants are used in another body part of the patient. However, the graft size that can be taken from the patient is limited. There is also a risk of infection and pain at the donor site following surgery [20, 22]. Bone tissue is more common than autograft tissue because it comes from dead and living sources, such as removing femoral heads in hip replacement surgery. Many studies in the literature exist to conduct BTE in developing alternatives to traditional bone grafts [23–25]. This is to compensate for the shortcomings of current treatment options. Various porous 3D scaffolds made from different biomaterials and constructed in multiple ways have been used to aid and guide bone regeneration. However, the scaffold material has yet to be discovered, and using 3D scaffolds in clinical settings is challenging. Bone is made up of the mineral calcium hydroxyapatite $\text{Ca}_{10}(\text{PO}_4)_6(\text{OH})_2$, an organic component mixture of lipids and non-collagenous proteins [26–28].

Inert materials, such as alumina and zirconia, are not absorbed by the body. Semi-inert materials, including glass ceramics, are bioactive or have a reactive surface, and non-inert materials break down. The body absorbs aluminates and calcium phosphates; ceramics are only used for bone implants, which do not need to be strong mechanically. Most shapes and properties can be found in artificial and natural polymers [14, 25, 29]. They are easier to work with and change than metals and ceramics. Therefore, they can make materials better or change how they work. Mixing polymers, ceramics, and metals can change biomaterials' physical-chemical, mechanical, and biological properties. High-strength composites can be made by putting ceramics in polymeric matrices [30–32]. Nanocomposites are made when the size of at least one dispersed particle is less than 100 nm. Biomaterials with a nanostructure are alternatives

to those with a macro- or microstructure because their properties might be better, and there is more interaction between their parts. Nanocomposites are used in dental fillings and orthopaedic implants. Even though a nanostructured biomaterial has micrometric dimensions, it may have nanometric properties [32–34].

Three additive manufacturing processes stand out in developing new products in the medical sector and research. Firstly, the fused deposition modelling (FDM) process uses a thermo-mouldable polymer as a raw material. It is melted when heated and deposited in successive layers to form the object. Secondly, stereolithography (SLA) is a process in which a photopolymer is solidified by an ultraviolet (UV) laser beam, creating the object. This process allows for high accuracy but costs high materials and equipment [33–35]. Thirdly, selective laser sintering (SLS) like the SLA process, but SLS has a slightly lower price and uses as raw material, a powder of thermoplastic materials, metal, ceramics, and others that can be composed [34–36]. The FDM process, created in the 1980s, was marketed by the American company Stratasys in the early 1990s. Several types of desktop 3D printers are available today, including national production, with prices ranging from \$120 to \$30,000 and employing the FDM process. A thermoplastic filament is heated and melted while passing through an extrusion head to manufacturing an object previously modelled on computer-aided design (CAD) software. This material is neatly deposited in successive layers on a platform through the extrusion nozzle. On most 3D printers, the extrusion nozzle moves along the x and y axes. In contrast, the print platform moves along the z axis [37]. Due to the typical characteristics of the FDM process, the parts produced in thermoplastic material present a significant variation in their material properties. The mechanical resistance between the layers is significantly lower than in the regions towards the x and y axes. Therefore, any attempt to improve the mechanical strength of parts made by the FDM process should be made, considering this fact [35, 36, 38].

Besides, the mechanical strength of the filament used in the FDM process is not the most critical parameter for determining the mechanical strength of the 3D-printed part. The strength and stability obtained between the part layers are determined by the print parameters, such as orientation, speed, and infill [38, 39]. Despite these limitations, the FDM process has been used to produce parts in various industry sectors due to its reliability, affordability, production effectiveness with good resolution and dimensional stability, the possibility of customisation, and the ability to manufacture complex geometries [36, 38, 39].

There are several previous works on the durability and strength of PEEK for a bone implant with and without calcium hydroxyapatite (cHAP) and description of their mechanical behaviours. There is, however, a missing link

between the coherent microstructure and the design of a compatible structure for a femur-implant of PEEK and cHAp composite. Also, the description of the process and its consequences within the context of mechanical behaviours, morphological changes, and prediction of elastic behaviour related to femur bone are scarce. Therefore, this study analyses and discusses the contemporary perspectives and development of femur-implant using polymeric and composite biomaterials. A significant way to fabricate biomaterials for medical uses, focusing on 3D printing, was proposed and evaluated. Afterwards, a novel method and solution for preparing polymer materials and scaffolds using FDM were presented. The properties of BTES were described by giving new designs and materials for the process of bone structure, emphasising polymer material frequently used in 3D printing technology, scaffold structure design optimisation, and clinical application. This study also described the technical challenges of current research and the potential prospects of 3D-printed polymer BTES. It produced a biomimetic femur-implant PEEK-cHAp composite scaffold for bone repair.

2 Materials and methods

Qingdao Freyr Graphite Company in China provided the -cHAp. The -cHAp composites were used to create epoxy, mixed with an identical epoxy ratio of 70:30 in various ratios of 0, 1, 3, and 5%. The composites were combined at 40 °C in an oven for 5 min at 25 °C [11, 36, 38] to remove the surface moisture, and the models were baked for 3.5 h at 40 °C. The epoxy reaction was completed after 48 h at an ambient temperature of 25 °C. The details, including percentage weight (wt%) and properties of the -cHAp, are presented in Table 1.

PEEK is a semi-crystalline, linear-chain organic thermoplastic with excellent performance and durability. It is biocompatible, stable chemically, and radiolucent and has the same elasticity as natural bone. It was initially used as a biomaterial to repair the knee and hip joints. These studies showed that PEEK is biologically inert, not interacting with living tissue due to its low bioactivity. Studies continue to change its surface to make it more bioactive. For example, particle leaching can change the roughness of the

polymer surface by creating pores, which makes it better at interacting with cells and tissues [39, 40]. The biocompatibility of PEEK composites was confirmed in in vitro cytotoxicity studies, in which the biomaterial caused a minimal inflammatory response and could be used for stimulation and integration with local tissue. Fig. 1 depicts the detailed and novel designs of different lattice structures considered within the scope of this study. They were slipt, lidinoin, diamond, and gyroid to mimic bone structures for femur-implant application. Besides, when comparing composites and characteristics in each volume, the density of PEEK-cHAp at 1310 kg/m³ is used as a reference. The modulus of elasticity for PEEK and cHAp is 3.85 Gpa and 10 Gpa, respectively, with a modulus of rigidity of 1.375 Gpa and 3.943 Gpa, respectively. The mechanical properties of femur’s trabecular bone have a density of 1.37 g/cm³, Young modulus of 3.195 Gpa, and Poisson’s ratio of 0.4 [41]

Modulus of elasticity of the new composite:

$$E_c = E_p V_p + E_{cHAp} V_{cHAp} = E_c = 3.85(0.7) + 10(0.3) = 5.695 \text{ Gpa}$$

Modulus of rigidity of the new composite:

$$G_c = G_p V_p + G_{cHAp} V_{cHAp} = G_c = 1.375(0.7) + 3.943(0.3) = 2.1454 \text{ Gpa}$$

Figure 1 shows the different lattices or shapes considered to establish the relevance of lattice/shape to the properties of the PEEK-based composite scaffold. The symbol represents the expected change in force, which occurs when it is used by the human.

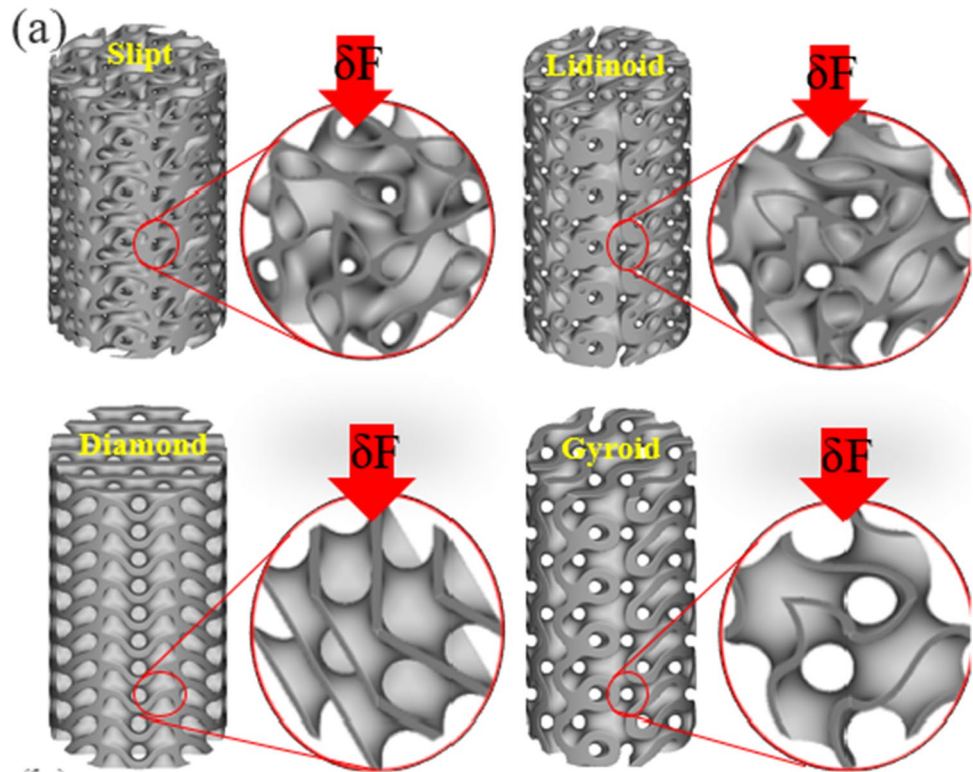
3 Biocompatibility study

In Dulbecco’s Modified Eagle Medium (DMEM) cultivation, cells were produced in the low glucose of 5/bag, foetal calf serum of 10%, penicillin/streptomycin of 1%, and GlutaMAX of 1% in the vials (Hyclone, Thermo, USA) were grown—sterile cultivations of 75 ml cells. The medium was an essential medium in which different mammoth cells were cultivated. DMEM offered four more amino acids and vitamins than the original eagle environment. Low-cost DMEM powder is easy to transport and store; L-glutamine phenol red with low

Table 1 PEEK and cHAp used, and their wt% and properties

PEEK (wt%)	cHAp (wt%)	Young modulus (E) GPa	Shear modulus (G) GPa	Bulk modulus (Gpa)	Poisson's Ratio	Lamé’s Constant λ (Gpa)
70.0	cHAp30	5.69	2.1454	5.453	0.33	4.023
80.0	cHAp20	5.08	1.8886	5.459	0.34	4.2
90.0	cHAp10	4.465	1.632	5.636	0.37	4.548
100	cHAp0	3.850	1.397	5.574	0.38	4.648
	Trabecular Bone	3.195	1.141	5.325	0.40	4.564

Fig. 1 Design of slipt, lidinoin, diamond, and gyroid to mimic bone structures



glucose levels of 1.0 g/L has little or no NaHCO_3 and sodium pyruvate. Cells were cultured at 37 °C in a humid atmosphere of 5% CO_2 . The thiazolyl blue tetrazolium bromide (MTT) assay was done to see how dangerous composite samples were to NIH-3T3 murine fibroblast cells. In 96-well plates, cells were seeded in high-glucose DMEM [16, 42, 43].

After 24 h of plating, different components suspended in a culture medium were added to the wells. At 35 °C, each well was filled with 20 L of MTT solution of 5 mg/mL in PBS, pH of 7.2, and the plates were incubated for 2 h at 35 °C. The medium was withdrawn, and each well was filled with dimethyl sulfoxide of 100 L and rapidly agitated to dissolve the formazan crystals. The absorbance of the formazan solutions was measured using a microplate reader at a wavelength of 595 nm in five repeats for each of the two sample concentrations. The absorbance ratio of the treated versus the untreated cells was used to calculate cytotoxicity, expressed as a percentage of cell viability.

4 Results and discussion

There was an increase in the grain size from an average diameter of 3.55 to 3.74 μm . Consequently, it affected the correlation and compatibility of the samples with the appearance of smaller spherical nanoparticles with a diameter ranging from 0.673 to 0.647 μm . This is suitable in tissue engineering applications.

Hence, this established additively manufactured/3D-printed PEEK-cHAp composite scaffolds as bone implants for biomimetic heterogeneous artificial bone repair. The sintered material presented a rough structure, suggesting high porosity and mechanical strength. With adequate knowledge of the biocompatibility of the construction of 800- μm pores using AM, tests were performed to obtain scaffolds in the additive manufacturing (AM) equipment. The platforms with pores of 500 μm were brought. Also, pores with 700 μm on the side and 500 μm on the wall were obtained in a mandibular bio-model. Other tests performed involved the construction of parts formed by the nylon-copper composite. In addition to the property of PEEK-cHAp as a biocompatible material, the experiments have demonstrated that polymer-metal composites were amenable to rapid prototype polymer or ceramic prototyping, as shown in Table 1 for biopolymers and cHAp. Figure 2 shows the consequence of 3D printing of bone implants, different triply periodic minimal surfaces (TPMS) lattice structures in FDM, and infill of the lattice structures of femur-implant scaffolds.

4.1 In vitro and microstructural analysis

The frequency spectrum parameters of the same wavelength measured in millimetres were 33.7, -48.9, and -40.8 dBc for the first, third, and seventh days, respectively. The grain particle slice was used to analyse the percentage projected area. The experimental mean densities of the furrows

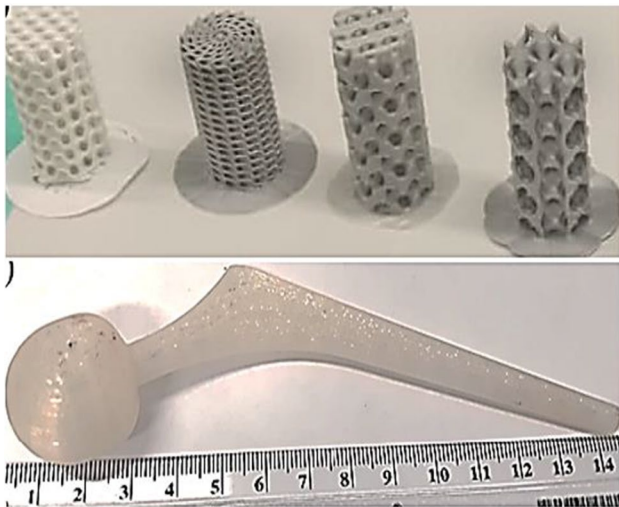


Fig. 2 The consequence of 3D printing of bone implant, different TPMS lattice structures in FDM, and infill of the designed lattice of femur-implant scaffold

measured were 3.65, 2.31, and 1.14 cm/cm², respectively. On the other hand, they have less mechanical resistance, especially with AM technology. Also, powder use offered the greatest geometric freedom among all the existing prototyping techniques since the powder supported manufacturing suspended and negatively inclined structures.

The build-up of cells in the surface profile was observed

scattered. Many actin filaments binding neighbouring cells were observed in the PEEK-cHAp combination. Also, cell nuclei in the PEEK-cHAp combination were denser when compared with the PEEK surfaces. From Fig. 3, the cells in the PEEK-cHAp complex clustered together, whereas those in the PEEK were scattered (Fig. 3). This can be attributed to the presence of -cHAp, causing the clustering of the cells during in vitro testing.

4.2 Biomaterial

Biomaterials from nanofibres are employed in controlled release, tissue engineering and regenerative medicine. People are interested in these materials because they have a high surface area, are mechanically flexible, are simple to manufacture, can have their surfaces altered, and have a structure that resembles physiological microenvironments in vivo. Due to their composition, form, and various topologies, such as coaxial fibres, nanofibres may alter the release rate of therapeutic agents, such as medicines, enzymes, and cells. Janus and coaxial fibres are intriguing because their internal and exterior features may be utilised to regulate how much of the active ingredient is delivered. The coaxial configuration also allows one or more medicinal drugs to be placed simultaneously in each layer of the fibres [44, 45]. The therapeutic substance may be released from the nanofibres in response to light, a magnetic field, an electric field, ultrasound, or temperature changes. The therapeutic agent dosage may be

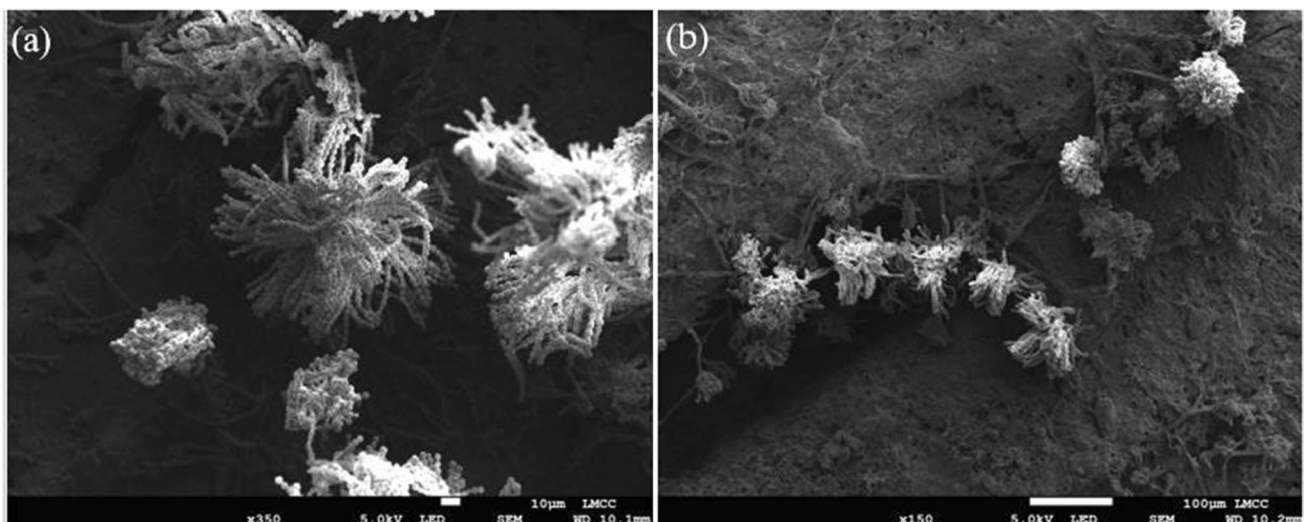


Fig. 3 SEM structures of PEEK-cHAp culture scaffold, showing both **a** PEEK and **b** PEEK-cHAp for 24 h

because of the mutual manufacturing process of the deposition layers (Fig. 3). The cells in the PEEK-cHAp complex clustered together, whereas those in the PEEK were

adjusted to fit the demands of each patient. This improves the treatment and reduces its harmful impact on the body. Nanofibres are helpful in regenerative medicine and tissue

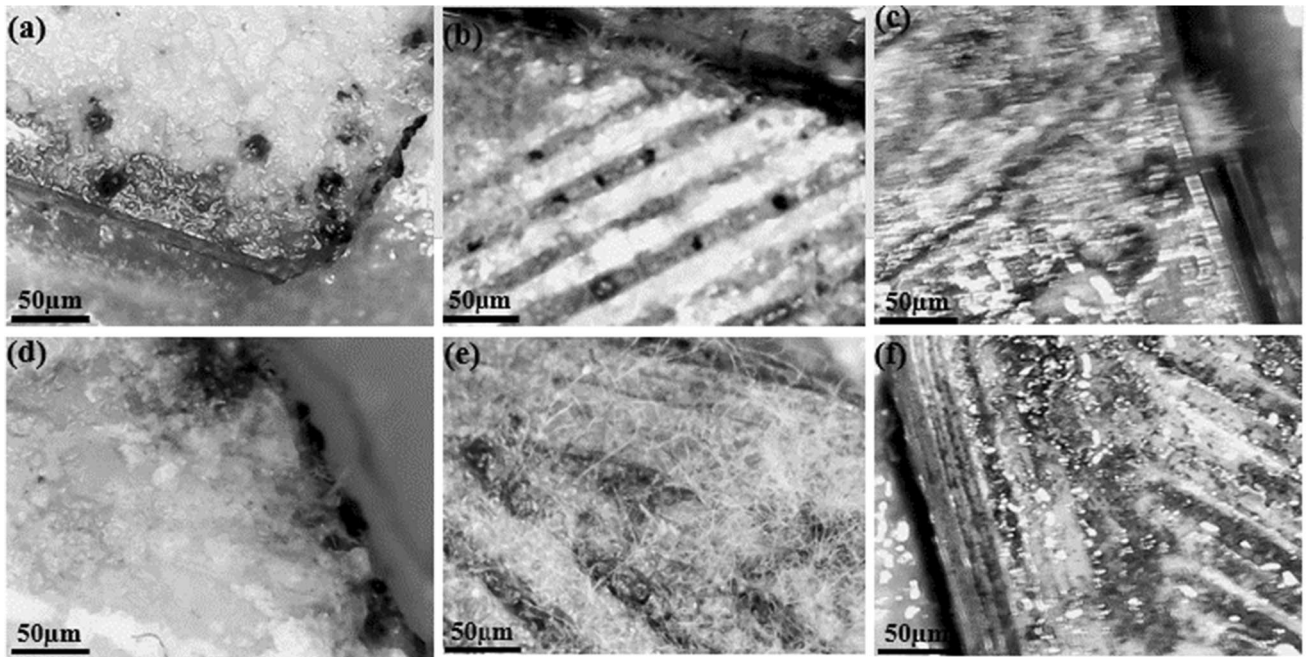
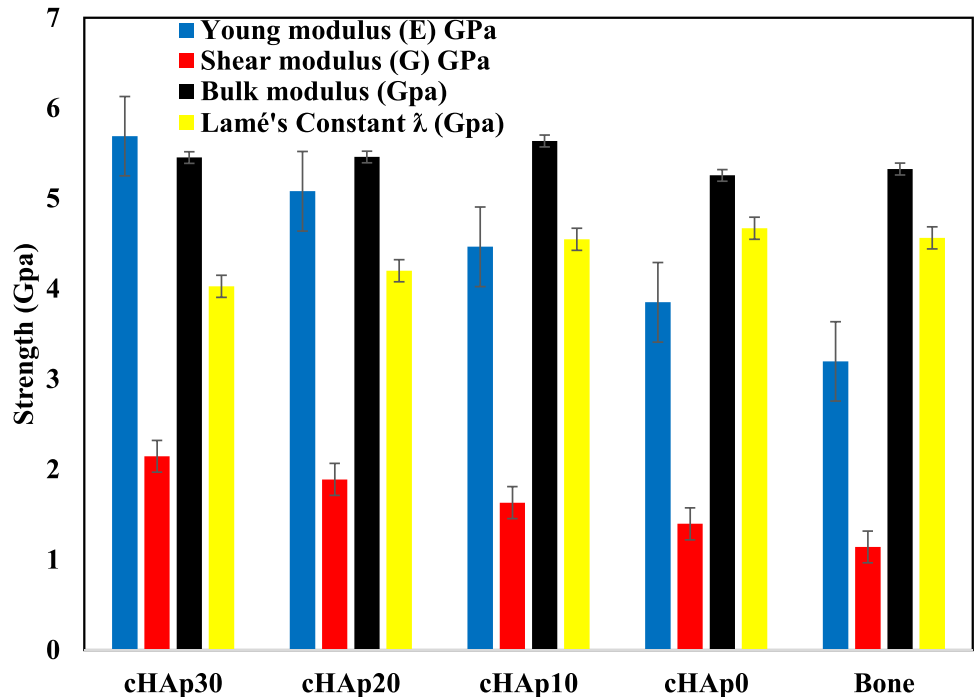


Fig. 4 Cells cultured with new active substance (NAS) and mounted to FDM 3D-printed: **a–c** PEEK composite sample surfaces, **c** stained by live/dead status at 50 μm, **d** live-cell growth on PEEK-cHAp, **e** increased cell activity on PEEK, and **f** PEEK on third day

engineering due to their porous nature and high surface ratio. They also resemble the extracellular matrix of several tissues. Fibres may be laid down in 3D structures and modified in composition, surface, mechanical characteristics, and degradability. Cells may develop in these structures and be employed to create functional units. Studies found that when immune system dendritic cells came in touch with fibres,

they did not alter or produce cytotoxins [46, 47]. They did not perceive the nanofibres as foreign bodies. Figure 4a–f depicts melanoma cells adhered to and moved about the PEEK nanofibres PEEK blends created by blow spinning. Nanofibres have been utilised to manufacture bandages and aid in regenerating cartilage, nerve, and heart tissue.

Fig. 5 The relative shear modulus of a human femur bone implant vs a composite's relative density is examined in tensile tests of lattice structures, composites, and post-mechanical strength



Furthermore, 3D fibre structures are used as support materials for in vitro models that mimic tissues, normal organs, and diseased microenvironments to model diseases, test drugs, and observe their toxicity. This method predicts how dangerous and effective medicines be without using animal models. This cuts down on the time and money needed to make new medicines. Nanobras are models of breast, prostate, pancreatic, and colorectal cancer tumours grown in a laboratory dish. They track how the disease spreads and restorative treatments work. Support materials made with a 3D printer might help cartilage and bone growth. After a tooth is pulled, polymeric nanocomposites and 3D-printed composites are used in implants to protect the alveoli in the maxilla and mandible. In engineering, bone tissue 3D printing is used for craniofacial reconstruction with these primary goals. Replacement is fixing a problem with a custom-made prosthesis [5, 48, 49]. This occurs when a large bone or soft tissue area is missing after an injury or tumour removal. Help is needed to restore bone by putting in bone grafts and ensuring they have structure and primary stability. Stimulate bone tissue involves regeneration to keep existing bone and osteogenesis to repair bone and restore normal anatomy and function.

3D printing can also simplify drug delivery systems, such as drug-eluting implants, medical devices, or pills, with the correct number of drugs for each patient. Now, creating different medicines that could not be made before is possible. This method is flexible because it can make medications with varying release profiles, including slow-release or fast-dissolving tablets or with a combination of more than one active principle [45, 50]. Bioprinting methods have made it possible to create prototypes of the whole organs, such as vascularised and heart tissue, with actin movement that mimics heartbeats and is compatible with the immune system of the patient, cells, biochemistry, and anatomy. When stem cells and 3D printing are used, the patient's liver cells can make tissue for implants. The cell activity results are shown in Fig. 4a–f; more activities and responses of the cells in 24 h (first), third, seventh, and 14th days are depicted in Fig. 4a–f.

The growth and response of the cells can be further observed and analysed from the computational 4D printing views of the scaffolds with change in time, as depicted in Fig. 5. The particle grain of each cell grew with time. The cell grain in PEEK that grew in DMEM was smaller than that in PEEK-cHAp, and the same was valid for the scaffold that grew in NAS. There were significant cultural cell grains in the seventh-day culture with NAS compared to the first day with a fine and smaller grain nanoparticle. Figure 5 compares the 3D-printed femur-implant scaffolds with a human femur regarding relative shear modulus versus composite relative density. Young's elastic and shear moduli of the composites increased with their weight percentages. The moduli were more than two times when compared with the human femur.

The composite scaffolds can be viable for biomimetic heterogeneous artificial bone regeneration, considering their relevance and application in biomedical or bone tissue engineering. In addition, Fig. 5 shows the results of the discrepancy between the strengths of the 3D-printed samples and the natural femur. However, the margin of error remained constant at about 5%. This is a massive clue that the tried-and-true porosity calculation approach can accurately estimate the porosity of the structures.

5 Conclusions

The results obtained from this study established that the 3D-printed PEEK-cHAp composite scaffolds manufactured through the FDM technique possessed excellent mechanical properties, good forming ability, and cytocompatibility. Hence, the following concluding remarks can be deduced.

As a result of the improved or better tensile strength, stiffness, and Young's moduli of the 3D-printed composites compared with the pure epoxy matrix, especially at cHAp of 10 and 20 wt%, they can be used as alternatives in bone tissue engineering, considering cHAp30 will make the composite too stiff.

Motif and furrow segmentation profoundly affected the grain size, and 3D morphology in PEEK-cHAp microstructure of particle size was reduced.

The importance of consistency and the composites' mechanical properties was evident from the results obtained. Also, the impact force improved with the addition of rGO-epoxy composites. Therefore, they are instrumental in the biomedical and bioengineering sectors.

Considering the optimum samples, the biomedical or bone tissue engineering application of the various improved FDM/3D-printed PEEK-cHAp composite scaffolds depends on their biological and mechanical properties, as the need for the femur and other bone implants remains indispensable.

Authors' contribution Bankole Oladapo: Conceptualisation, methodology, software, writing (original draft), validation. Abolfazl Zahedi: Writing (review and editing), visualisation, investigation. Sikiru Ismail: Writing (review and editing), supervision. Wattala Fernando: Review and editing, funding acquisition. Omolayo Ikumapayi: Review and editing, validation.

Declarations

Conflict of interest The authors declare no competing interests.

Open Access This article is licensed under a Creative Commons Attribution 4.0 International License, which permits use, sharing, adaptation, distribution and reproduction in any medium or format, as long as you give appropriate credit to the original author(s) and the source, provide a link to the Creative Commons licence, and indicate if changes were made. The images or other third party material in this article are included in the article's Creative Commons licence, unless indicated

otherwise in a credit line to the material. If material is not included in the article's Creative Commons licence and your intended use is not permitted by statutory regulation or exceeds the permitted use, you will need to obtain permission directly from the copyright holder. To view a copy of this licence, visit <http://creativecommons.org/licenses/by/4.0/>.

References

- Bhimasankaram T, Suryanarayana SV, Prasad G (1998) Piezoelectric polymer composite materials. *Curr Sci*:967–976
- Behera K, Sivanjineyulu V, Chang Y-H, Chiu F-C (2018) Thermal properties, phase morphology and stability of biodegradable PLA/PBSL/HAp composites. *Polym Degrad Stab* 154:248–260. <https://doi.org/10.1016/j.polymdegradstab.2018.06.010>
- Gong F, Bui K, Dv P, Hm D (2014) Thermal transport phenomena and limitations in heterogeneous polymer composites containing carbon nanotubes and inorganic nanoparticles. *Carbon (New York)* 78:305–316. <https://doi.org/10.1016/j.carbon.2014.07.007>
- Caminero MÁ, Chacón JM, García-Plaza E, Núñez PJ, Reverte JM, Becar JP (2019) Additive Manufacturing of PLA-Based Composites Using Fused Filament Fabrication: Effect of Graphene Nanoplatelet Reinforcement on Mechanical Properties. *Dimens Acc Tex Polym* 11:799. <https://doi.org/10.3390/polym11050799>
- Dey SK, Chatterjee S, Spieckermann F, Ghosh P, Samanta S (2019) Reversing and non-reversing effects of PEEK-HA composites on tuning cooling rate during crystallisation. *J Polym Res* 26:1–16. <https://doi.org/10.1007/s10965-019-1967-2>
- Gao S-L, Kim J-K (2002) Correlation among crystalline morphology of PEEK, interface bond strength, and in-plane mechanical properties of carbon/PEEK composites. *J Appl Polym Sci* 84:1155–1167. <https://doi.org/10.1002/app.10406>
- Falahati M, Ahmadvand P, Safaee S, Chang Y-C, Lyu Z, Chen R et al (2020) Smart polymers and nanocomposites for 3D and 4D printing. *Mater Today* 40:215–245
- Guo C, Liu X, Liu G (2021) Surface finishing of FDM-fabricated amorphous polyetheretherketone and its carbon-fiber-reinforced composite by dry milling. *Polymers* 13:2175. <https://doi.org/10.3390/polym13132175>
- Melčová V, Svoradová K, Menčík P, Kontárová S, Rampichová M, Hedvičáková V et al (2020) FDM 3D printed composites for bone tissue engineering based on plasticised poly(3-hydroxybutyrate)/poly(d,l-lactide) blends. *Polymers* 12:2806. <https://doi.org/10.3390/polym12122806>
- Turnbull G, Clarke J, Picard F, Riches P, Jia L, Han F et al (2018) 3D bioactive composite scaffolds for bone tissue engineering. *Bioact Mater* 3:278–314. <https://doi.org/10.1016/j.bioactmat.2017.10.001>
- Heimer S, Schmidlin PR, Stawarczyk B (2017) Discoloration of PMMA, composite, and PEEK. *Clin Oral Investig* 21:1191–1200. <https://doi.org/10.1007/s00784-016-1892-2>
- Oladapo BI, Kayode JF, Karagiannidis P, Naveed N, Mehrabi HA, Ogundipe KO (2022) Polymeric composites of cubic-octahedron and gyroid lattice for biomimetic dental implants. *Mater Chem Phys* 126454. <https://doi.org/10.1016/j.matchemphys.2022.126454>
- Dai G, Zhan L, Guan C, Huang M (2020) The effect of moulding process parameters on interlaminar properties of CF/PEEK composite laminates. *High Perform Polym* 32:835–841. <https://doi.org/10.1177/0954008320903768>
- Flanagan M, Grogan DM, Goggins J, Appel S, Doyle K, Leen SB et al (2017) Permeability of carbon fibre PEEK composites for cryogenic storage tanks of future space launchers. *Compos Part A Appl Sci Manuf* 101:173–184. <https://doi.org/10.1016/j.compositesa.2017.06.013>
- Mehta R, Chhibber R, Kumar SS (2018) PEEK Composite Scaffold Preparation for Load Bearing Bone Implants. *Mater Sci Forum* 911:77–82. <https://doi.org/10.4028/www.scientific.net/MSF.911.77>
- Garcia-Gonzalez D, Rusinek A, Jankowiak T, Arias A (2015) Mechanical impact behavior of polyether-ether-ketone (PEEK). *Compos Struct* 124:88–99. <https://doi.org/10.1016/j.compstruct.2014.12.061>
- Oladapo BI, Ismail SO, Bowoto OK, Omigbodun FT, Olawumi MA, Muhammad MA (2020) Lattice design and 3D-printing of PEEK with Ca10(OH)(PO4)3 and *in-vitro* bio-composite for bone implant. *Int J Biol Macromol* 165:50–62. <https://doi.org/10.1016/j.ijbiomac.2020.09.175>
- Oladapo BI, Zahedi SA, Ismail SO, Omigbodun FT (2021) 3D printing of PEEK and its composite to increase biointerfaces as a biomedical material- A review. *Colloids Surf B: Biointerfaces* 111726. <https://doi.org/10.1016/j.colsurfb.2021.111726>
- Lin L, Schlarb AK (2019) Recycled carbon fibers as reinforcements for hybrid PEEK composites with excellent friction and wear performance. *Wear* 432–433:202928. <https://doi.org/10.1016/j.wear.2019.202928>
- Oladapo BI, Zahedi SA, Ismail SO, Omigbodun FT (2021) 3D printing of PEEK and its composite to increase biointerfaces as a biomedical material- A review. *Colloids Surf B Biointerfaces* 203:111726. <https://doi.org/10.1016/j.colsurfb.2021.111726>
- Liang Y, Gao D, Chen B, Zhao J (2019) Friction and Wear Study on Friction Pairs with a Biomimetic Non-smooth Surface of 316L Relative to CF/PEEK under a Seawater Lubricated Condition. *Chinese J Mech Eng* 32:1–14. <https://doi.org/10.1186/s10033-019-0380-4>
- Oladapo BI, Zahedi SA, Adeoye AOM (2019) 3D printing of bone scaffolds with hybrid biomaterials. *Compos Part B* 158:428–436
- Oladapo BI, Zahedi SA (2021) Improving bioactivity and strength of PEEK composite polymer for bone application. *Mater Chem Phys* 266:124485
- Xu Y, Zhang F, Zhai W, Cheng S, Li J, Wang Y (2022) Unraveling of Advances in 3D-Printed Polymer-Based Bone Scaffolds. *Polymers (Basel)* 14:566. <https://doi.org/10.3390/polym14030566>
- Oladapo BI, Zahedi SA, Ismail SO, Omigbodun FT, Bowoto OK, Olawumi MA et al (2021) 3D printing of PEEK–cHAp scaffold for medical bone implant. *Bio-Des Manuf* 4:44–59
- Lai W, Wang Y, Fu H, He J (2020) Hydroxyapatite/polyetheretherketone nanocomposites for selective laser sintering: Thermal and mechanical performances. *E-Polymers* 20:542–549. <https://doi.org/10.1515/epoly-2020-0057>
- Oladapo BI, Zahedi SA, Ismail SO, Olawade DB (2021) Recent advances in biopolymeric composite materials: Future sustainability of bone-implant. *Renew Sust Energ Rev* 150:111505. <https://doi.org/10.1016/j.rser.2021.111505>
- Perumal S, Atchudan R, Cheong IW (2021) Recent Studies on Dispersion of Graphene-Polymer Composites. *Polymers* 13:2375. <https://doi.org/10.3390/polym13142375>
- Oladapo BI, Balogun V (2016) Electrical energy demand modeling of 3D printing technology for sustainable manufacture. *Int J Eng* 29:954–961
- Oladapo BI, Daniyan IA, Ikumapayi OM, Malachi OB, Malachi IO (2020) Microanalysis of hybrid characterisation of PLA/cHA polymer scaffolds for bone regeneration. *Polym Test* 83:106341. <https://doi.org/10.1016/j.polymertesting.2020.106341>
- Oladapo BI, Ismail SO, Ikumapayi OM, Karagiannidis PG (2022) Impact of rGO-coated PEEK and lattice on bone implant. *Colloids Surf B: Biointerfaces* 112583. <https://doi.org/10.1016/j.colsurfb.2022.112583>
- Feng P, Jia J, Peng S, Yang W, Bin S, Shuai C (2020) Graphene oxide-driven interfacial coupling in laser 3D printed PEEK/PVA scaffolds for bone regeneration. *Virtual and Physical Prototyping* 15:211–226. <https://doi.org/10.1080/17452759.2020.1719457>
- Souza JCM, Correia MST, Henriques B, Novaes de Oliveira AP, Silva FS, Gomes JR (2019) Micro-scale abrasion wear of novel biomedical

- PEEK-matrix composites for restorative dentistry. *Surf Topogr Metr Prop* 7:15019. <https://doi.org/10.1088/2051-672X/ab0324>
34. Oladapo BI, Ismail SO, Zahedi M, Khan A, Usman H (2020) 3D printing and morphological characterisation of polymeric composite scaffolds. *Eng Struct* 216:110752. <https://doi.org/10.1016/j.engstruct.2020.110752>
 35. Oladapo BI, Zahedi SA, Vahidnia F, Ikumapayi OM, Farooq MU (2018) Three-dimensional finite element analysis of a porcelain crowned tooth. *Beni-Suef University J Basic Appl Sci* 7:461–464
 36. Gaal G, Gaal V, Braunger ML, Riul A, Rodrigues V (2020) FDM 3D Printing in Biomedical and Microfluidic Applications. In: *3D Printing in Biomedical Engineering*. Singapore: Springer, Singapore, pp 127–145. https://doi.org/10.1007/978-981-15-5424-7_6
 37. Jin Y, Li H, He Y, Fu J-Z (2015) Quantitative analysis of surface profile in fused deposition modelling. *Addit Manuf* 8:142–148. <https://doi.org/10.1016/j.addma.2015.10.001>
 38. Arif MF, Alhashmi H, Varadarajan KM, Koo JH, Hart AJ, Kumar S (2020) Multifunctional performance of carbon nanotubes and graphene nanoplatelets reinforced PEEK composites enabled via FFF additive manufacturing. *Composites Part B. Eng* 184:107625. <https://doi.org/10.1016/j.compositesb.2019.107625>
 39. Oladapo BI, Zahedi SA, Balogun VA, Ismail SO, Samad YA. Overview of additive manufacturing biopolymer composites 2021.
 40. Oladapo BI, Obisesan OB, Oluwole B, Adebisi VA, Usman H, Khan A (2020) Mechanical characterisation of a polymeric scaffold for bone implant. *J Mater Sci* 55:9057–9069
 41. Gautam D, Rao VKP (2021) Nondestructive Evaluation of Mechanical Properties of Femur Bone. *J Nondestruct Eval* 40:22. <https://doi.org/10.1007/s10921-021-00754-0>
 42. Darwich A, Nazha H, Abbas W (2019) Numerical study of stress shielding evaluation of hip implant stems coated with composite (carbon/PEEK) and polymeric (PEEK) coating materials. *Biomed Res* 30. <https://doi.org/10.35841/biomedicalresearch.30-18-1048>
 43. Li W, Kang J, Yuan Y, Xiao F, Yao H, Liu S et al (2016) Preparation and characterisation of PVA-PEEK/PVA- β -TCP bilayered hydrogels for articular cartilage tissue repair. *Compos Sci Technol* 128:58–64. <https://doi.org/10.1016/j.compscitech.2016.03.013>
 44. Oladapo BI, Ismail SO, Afolalu TD, Olawade DB, Zahedi M (2021) Review on 3D printing: Fight against COVID-19. *Mater Chem Phys* 258:123943
 45. Anguiano-Sanchez J, Martinez-Romero O, Siller HR, Diaz-Elizondo JA, Flores-Villalba E, Rodriguez CA (2016) Influence of PEEK Coating on Hip Implant Stress Shielding: A Finite Element Analysis. *Comput Math Methods Med* 2016:6183679–6183610. <https://doi.org/10.1155/2016/6183679>
 46. Oladapo BI, Adebisi AV, Elemure EI (2021) Microstructural 4D printing investigation of ultra-sonication biocomposite polymer. *J King Saud University-Eng Sci* 33:54–60
 47. Elawadly T, Radi IAW, El Khadem A, Osman RB (2017) Can PEEK be an implant material? Evaluation of surface topography and filled versus unfilled PEEK wettability with different surface roughness. *J Oral Implantol* 43:456–461. <https://doi.org/10.1563/aaid-joi-D-17-00144>
 48. Oladapo BI, Kayode JK, Akinyoola JO, Ikumapayi OM (2023) Shape memory polymer review for flexible artificial intelligence materials of biomedical. *Mater Chem Phys* 293, 126930. <https://doi.org/10.1016/j.matchemphys.2022.126930>
 49. Du Y-W, Zhang L-N, Ye X, Nie H-M, Hou Z-T, Zeng T-H et al (2015) In-vitro and in-vivo evaluation of bone morphogenetic protein-2 (BMP-2) immobilised collagen-coated polyetheretherketone (PEEK). *Front Mater Sci* 9:38–50. <https://doi.org/10.1007/s11706-015-0276-x>
 50. Canel T, Bağlan İ, Sınmazçelik T (2020) Mathematical modeling of heat distribution on carbon fiber poly (ether-ether-ketone) (PEEK) composite during laser ablation. *Opt Laser Technol* 127:106190. <https://doi.org/10.1016/j.optlastec.2020.106190>

Publisher's note Springer Nature remains neutral with regard to jurisdictional claims in published maps and institutional affiliations.